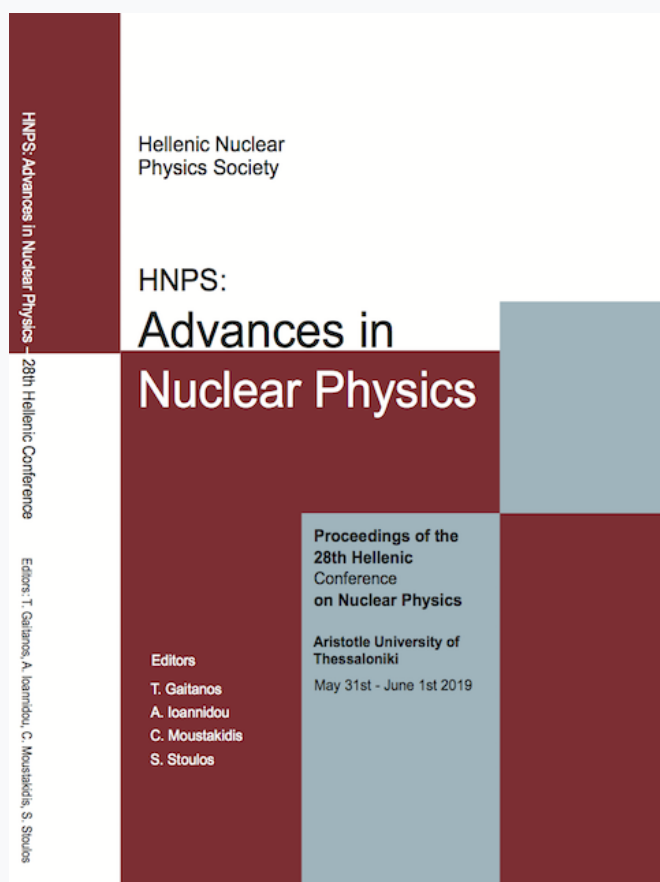


## Annual Symposium of the Hellenic Nuclear Physics Society

Τόμ. 27 (2019)

HNPS2019



### Constraints on neutron stars equation of state using the tidal deformability derived from BNS mergers

*Alkiviadis Kanakis-Pegios, Charalampos Moustakidis*

doi: [10.12681/hnps.2989](https://doi.org/10.12681/hnps.2989)

### Βιβλιογραφική αναφορά:

Kanakis-Pegios, A., & Moustakidis, C. (2020). Constraints on neutron stars equation of state using the tidal deformability derived from BNS mergers. *Annual Symposium of the Hellenic Nuclear Physics Society*, 27, 95–100. <https://doi.org/10.12681/hnps.2989>

# Constraints on neutron stars equation of state using the tidal deformability derived from BNS mergers

A. Kanakis–Pegios and Ch.C. Moustakidis

*Department of Theoretical Physics, Aristotle University of Thessaloniki, Greece*

**Abstract** *The purpose of this work is the study of neutron stars (NS) equation of state (EOS) using constraints on tidal deformability derived from observation of binary neutron star (BNS) mergers, such as GW170817. The mathematical formalism is introduced, and then for a variety of EOS the system is solved numerically, allowing us to determine the mass, the radius, the tidal love number  $k_2$  and the tidal deformability  $\lambda$  of the NS, each one of them unique for each EOS. Moreover, for a fixed value of chirp mass  $M_{\text{chirp}} = 1.188 M_{\odot}$  under the assumption that  $m_2 < m_1$  (where  $m_1$  is the heavier component mass of BNS system), the effective (mass-weighted) tidal deformability  $\tilde{\Lambda}$  of the binary system is determined for each EOS. We consider an upper limit of  $\tilde{\Lambda} \leq 800$  (GW170817) and a lower limit of  $\tilde{\Lambda} \geq 400$  (AT2017gfo). Also, we construct the  $\Lambda_1 - \Lambda_2$  space and we compare the behavior of EOS with the most recent LIGO's data. We found out that the most EOS models give values of  $\tilde{\Lambda}$  less than the upper limit and that the most stiff EOS are excluded.*

**Keywords** *neutron stars, gw170817, tidal deformability, equation of state*

*Corresponding author: A. Kanakis–Pegios (alkanaki@auth.gr) | Published online: May 1st, 2020*

## INTRODUCTION

On August 17, 2017, the LIGO & VIRGO gravitational waves (GW) detectors network observed a signal of emitted gravitational waves, from the inspiral of two compact objects, which was identified as a binary neutron star system (BNS). The contribute arising from the presence of VIRGO was determinant in order to strongly constraint the sky location of the source via triangulation-based techniques. The combined data from both LIGO and VIRGO detectors, determined the precise sky position of the source to an area of  $28 \text{ deg}^2$  [1]. This information enabled strong search, in the next days and weeks after the detection, for the optical and electromagnetic (EM) counterpart of the event.

Flanagan and Hinderer articulated that binary neutron stars coalescence is one of the most important source for gravitational waves detectors [2]. One of the goals of neutron stars (NS) binaries detections is to obtain informations about the nuclear equation of state (EoS). For the most part of the inspiral, finite-size effects have a negligible influence on the gravitational-wave signal, therefore only during the last orbits of the inspiral, and especially for GW frequencies above a lower limit of 500 Hz, the effect of the internal structure can be seen.

Some of the parameters that can be measured and constrained by the GW detectors are the chirp mass of the BNS and the effective tidal deformability. In the present work, we compute the mass, the radius and the tidal parameters of a single neutron star using the TOV equations for a variety of EoSs. Moreover, we use the constraints on the effective tidal deformability, that the GW170817 provided us, both from the GW signal and the EM counterpart, in order to study the behavior of each EoS.

## TIDAL EFFECTS

It has been shown that the orbital motion of a BNS system produced the emission of gravitational



waves, which removes energy and angular momentum from the system [2-4]. This causes the orbits to decrease in radius and increase in frequency, leading to the inspiraling motion of the two compact objects of the binary. During the late phase of the inspiral, the tidal interaction between the two compact bodies has a significant role to their gravitational field and orbital motion.

The induced tidal field  $E_{ij}$  affects the quadrupole moment  $Q_{ij}$ , and it's described by [5]:

$$Q_{ij} = \lambda(m)E_{ij},$$

where  $\lambda$  is the tidal deformability parameter, given by [5]:

$$\lambda = \frac{2}{3}k_2 \frac{R^5}{G} \quad (1)$$

The tidal deformability  $\lambda$  depends on the tidal parameter  $k_2$  and the radius  $R$ . The dependence on the star's radius means that the smaller the star, the harder to be deformed. The tidal parameter  $k_2$ , known as tidal love number, depends on the structure of the neutron star, i.e. its mass and equation of state, given by [5,6]:

$$k_2 = (\beta, y_R) = \frac{8\beta^5}{5}(1 - 2\beta)^2[2 - y_R + 2\beta(y_R - 1)] \times [2\beta(6 - 3y_R + 3\beta(5y_R - 8)) + 4\beta^3(13 - 11y_R + \beta(3y_R - 2) + 2\beta^2(1 + y_R)) + 3(1 - 2\beta)^2[2 - y_R + 2\beta(y_R - 1)] \ln(1 - 2\beta)]^{-1} \quad (2)$$

where  $\beta$  is the compactness of the star and  $y_R$  is a parameter which is determined as [5,6]:

$$r \frac{dy(r)}{dr} + y^2(r) + y(r)F(r) + r^2Q(r) = 0, \quad \text{with } y(0) = 2, y_R \equiv y(R) \quad (3)$$

$F(r)$  and  $Q(r)$  are functionals of the energy density, the pressure and the mass defined as [6]:

$$F(r) = \left[ 1 - \frac{4\pi r^2 G}{c^4} (\mathcal{E}(r) - P(r)) \right] \left( 1 - \frac{2M(r)G}{rc^2} \right)^{-1}$$

$$r^2 Q(r) = \frac{4\pi r^2 G}{c^4} \left[ 5\mathcal{E}(r) + 9P(r) + \frac{\mathcal{E}(r) + P(r)}{\partial P(r) / \partial \mathcal{E}(r)} \right] \left( 1 - \frac{2M(r)G}{rc^2} \right)^{-1}$$

$$- 6 \left( 1 - \frac{2M(r)G}{rc^2} \right)^{-1}$$

$$- \frac{4M^2(r)G^2}{r^2 c^4} \left( 1 + \frac{4\pi r^3 P(r)}{M(r)c^2} \right)^2 \left( 1 - \frac{2M(r)G}{rc^2} \right)^{-2}$$

The numerical integration of the previous equations, combined with the well known TOV equations, provide us the mass  $M$ , the radius  $R$  and the parameter  $y_R$ . Hence, the compactness parameter  $\beta$  and the tidal love number  $k_2$  can be determined for each equation of state.

In Fig. 2 we present the tidal deformability  $\lambda$  of a single neutron star as a function of its mass  $M$ . In general, the more stiff equations of state lead to bigger values for the tidal deformability. But even if an EoS provide a big value for the maximum mass, as we can see from Fig. 1, this is not enough to provide big value for the  $\lambda$ . For example, the HLPS-2 EoS predict big maximum mass for the NS, but too small values for the tidal deformability, regarding to other EoSs with smaller maximum masses. This behavior is due to the fact that  $\lambda$  is proportional to the 5-th power of star's radius, therefore is more sensitive to the radius than to the mass of the star, see Eq. (1).

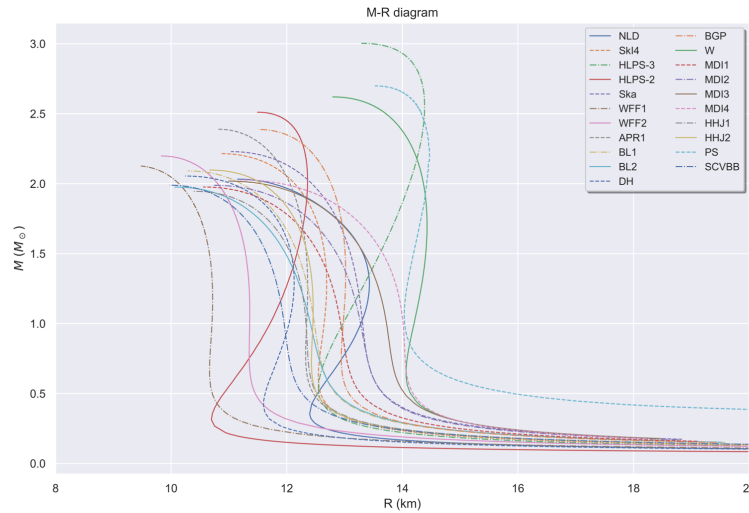


**Figure 1.** Mass vs Radius of a single NS, for various EoSs.

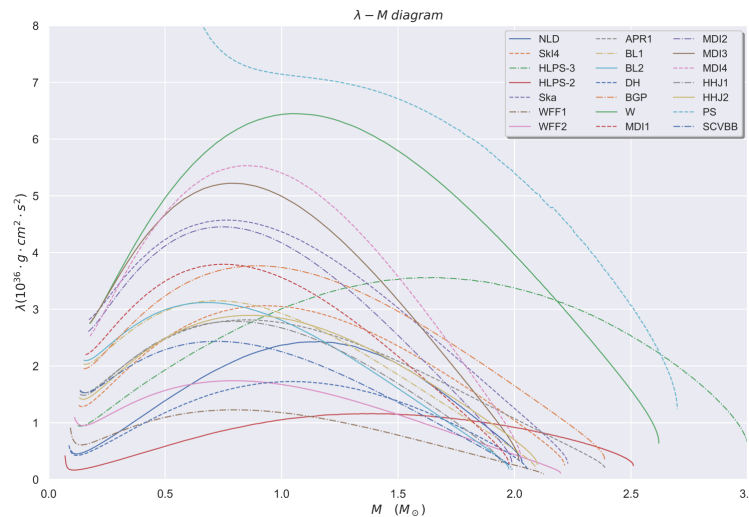


**Figure 2.** Tidal deformability  $\lambda$  of a single NS as a function of the mass  $M$ , for various EoSs.

## BINARY TIDAL DEFORMABILITY

We talked in the previous section about the significance of the tidal deformability in the late phase of evolution for a binary neutron star system. One of the parameters of the BNS that can be measured from the GW detector is the *chirp mass*  $\mathcal{M}_c$  [1]. The *chirp mass* is a quantity that contains the masses of the two component stars. Its exact form is given by [1]:

$$\mathcal{M}_c = \frac{(m_1 m_2)^{3/5}}{(m_1 + m_2)^{1/5}} = \frac{q^{3/5}}{(1 + q)^{1/5}} m_1 \quad (4)$$

where  $q = m_2/m_1$ , with  $m_2 \leq m_1 \rightarrow q \leq 1$ , is the *binary mass ratio*.

In addition, the combined tidal effects of two neutron stars in a circular orbits are given by a weighted (effective) average of the quadrupole responses [5,7], named *effective tidal deformability*, given by:

$$\tilde{\lambda} = \frac{1}{26} \left[ \frac{m_1 + 12m_2}{m_1} \lambda_1 + \frac{m_2 + 12m_1}{m_2} \lambda_2 \right] \quad (5)$$

We can rewrite Eq. (5) in a more appropriate way, in order to be a *dimensionless* quantity [8]:

$$\tilde{\Lambda} = \frac{16(12q + 1)\Lambda_1 + (12 + q)q^4\Lambda_2}{13(1 + q)^5} \quad (6)$$

where  $\Lambda = \lambda/M^5 = \frac{2}{3}k_2 \left(\frac{c^2 R}{GM}\right)^5$  is the *dimensionless tidal deformability* of a single NS.

The GW detectors provide strong constraints on the effective tidal deformability  $\tilde{\Lambda}$ . The GW170817 event puts an upper bound of about 800 (newer analysis of the signal from the LIGO gives a smaller upper limit), for a measured chirp mass  $\mathcal{M}_c = 1.188M_\odot$  and  $q \in (0.7, 1)$  [1]. The mass range for the heavier component star is  $m_1 = (1.36, 1.60)M_\odot$ , and for the lighter one is [1]:

$$m_2 = (1.17, 1.36)M_\odot$$

In our study we adopt the proposed values and ranges of parameters by LIGO, except for  $q$  ( $q \in (0.4, 1)$ ). By using the Eq. (6), for a fixed value of  $\mathcal{M}_c$ , one can determine the  $\tilde{\Lambda}$  (see Fig. 3).

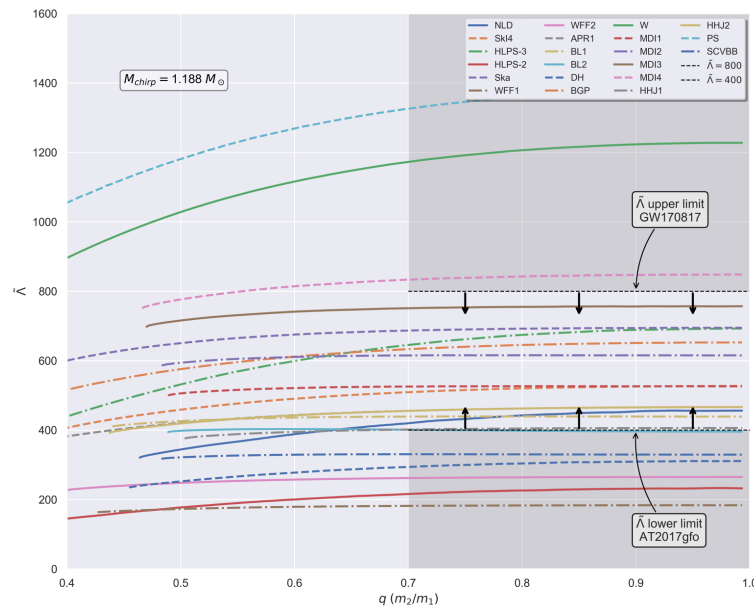


**Figure 3.**  $\tilde{\Lambda} - q$  relation for  $q \in (0.4, 1)$ ,  $\mathcal{M}_c = 1.188 M_\odot$  for various EoSs. The shaded grey color corresponds to the excluded regions from the analysis of the GW170817 signal (both from GW and EM counterparts). The upper limit on  $\tilde{\Lambda}$  is obtained from the LIGO/VIRGO analysis of the GW counterpart [1], while the lower limit is derived from the EM counterpart [9].

In Fig. 3 we show the effective tidal deformability  $\tilde{\Lambda}$  as a function of the binary mass ratio  $q$ . One can observe that the more stiff equations of state the bigger the values for  $\tilde{\Lambda}$ , in some cases even above the upper limit of 800. On the other hand, the more soft EoS, in general, the smaller the values for  $\tilde{\Lambda}$ . We note that the proposed value of the lower bound is still very wide (other studies propose different lower bound [9]), instead of the upper bound which is more tight.

Lattimer *et al* referenced that for masses  $m \geq 1M_\odot$ , the  $k_2$  parameter varies roughly as  $\beta^{-1}$  [8,10]. Under this assumption the dimensionless tidal deformability can be rewritten as:

$$\Lambda \simeq \alpha\beta^{-6} \quad (7)$$

where  $\alpha$  estimated to be  $\alpha = 0.0039 \pm 0.0007$  for the case of GW170817 event [10]. This value holds for masses in the range of  $1.1M_\odot \leq m \leq 1.6M_\odot$ , which is valid for the mass range of GW170817. As Soumi De *et al* pointed out [8], the range of stellar radii in the mass range of interest for GW170817 is small. Hence, because of the small mass sensitivity to the radius, it could be taken that  $R_1 \simeq R_2 \simeq \hat{R}$ . Therefore, by using the Eq.(7), it was found that [8,10]:

$$\Lambda_1 = q^6\Lambda_2 \quad (8)$$

By combining the Eq. (8) and Eq. (6), one can obtain that [8]:

$$\Lambda_1(\tilde{\Lambda}, q) = \frac{13}{16} \tilde{\Lambda} \frac{q^2(1+q)^4}{12q^2 - 11q + 12} \quad (9)$$

$$\Lambda_2(\tilde{\Lambda}, q) = q^{-6} \Lambda_1 \quad (10)$$

It is well known that when the two components have equal masses,  $m_1 = m_2 \rightarrow q = 1$ , then  $\tilde{\Lambda} = \Lambda_1 = \Lambda_2$  [8]. Therefore, for the given mass range of GW170817 event, one can compute the value of  $\tilde{\Lambda}$  when  $q = 1$  ( $m_1 = m_2 = 1.36 M_\odot$ ). Then, by treating the  $\tilde{\Lambda}$  as a constant, and for a specific range for  $q$ , the  $\Lambda_1, \Lambda_2$  can be computed from Eq. (9) and (10), for each EoS. Hence, the  $\Lambda_1 - \Lambda_2$  space can be constructed (see Fig. 4).

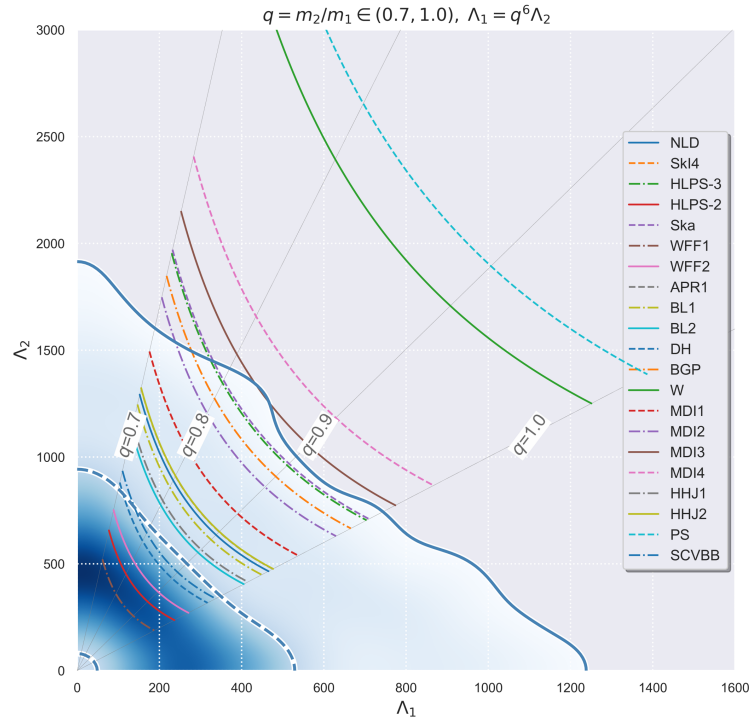


**Figure 4.**  $\Lambda_1 - \Lambda_2$  space for various EoS. The blue shaded color corresponds to the region of PhenomPNRT model's data [11,12]. The solid line corresponds to the 90% credible region, while the dashed line to the 50%. The overlaid grey lines correspond to different values of  $q$ .

In Fig. 4 we present the  $\Lambda_1 - \Lambda_2$  space for all the EoS that we used so far in our study. One can note that as in Fig. 3, the more stiff EoS in general are above the upper confidence limit of 90%, predicting large values for the  $\Lambda_1, \Lambda_2$ . These EoS are those with the bigger radii. This is not unexpected if we remind ourselves the dependence of  $\Lambda$  to the 5<sup>th</sup> order of  $R$ . Also, from the studying of Fig. 4 we note that the GW170817 event favors more compact neutron stars.

## DISCUSSION AND CONCLUSIONS

The EoS that we used in our analysis are consistent with the observational constraints on the maximum mass of neutron stars and reproduce a NS of  $2 M_\odot$ . In the first part of our work, we studied the mass, the radius and the tidal parameters for a single neutron star. We saw that in general the more stiff equations of state predict bigger values for the tidal deformability  $\lambda$ . In addition, we observed the significant role of the radius affecting the tidal deformability, both in a single neutron star and in the

binary case. Subsequently, we investigated the binary tidal parameters, especially the effective  $\tilde{\Lambda}$ . In our approach we adopted the estimations of the LIGO analysis regarding to the parameters of our interest. The GW170817 provided a strong constraint on the upper limit of  $\tilde{\Lambda}$ , while the lower limit is not specific. We used a value derived from the EM counterpart of the signal. The upper limit on the  $\tilde{\Lambda}$  led to the exclusion of the most stiff EoS. Also, by the studying of  $\Lambda_1 - \Lambda_2$  space one can note that the GW170817 event favors more compact neutron stars. We note that the detection of a BNS merger and the constraints that it brought to the EoS, it's only the beginning of a new era and further detections of future events will provide even more constraints on the equation of state and information to our knowledge about the neutron stars structure and characteristics.

## ACKNOWLEDGMENTS

The authors thank Prof. K. Kokkotas for his constructive comments on the preparation of the manuscript. This work was partially supported by the COST action PHAROS (CA16214) and the DAAD Germany-Greece grant ID 57340132.

## References

- [1] B.P. Abbott et al. (Virgo, LIGO Scientific), Phys. Rev. Lett. 119, 161101 (2017), doi: 10.1103/PhysRevLett.119.161101
- [2] E.E. Flanagan and T. Hinderer, Phys. Rev. D 77, 021502 (2008), doi: 10.1103/PhysRevD.77.021502
- [3] T. Binnington and E. Poisson, Phys. Rev. D 80, 084018 (2009), doi: 10.1103/PhysRevD.80.084018
- [4] T. Hinderer, Astrophys. J. 677, 1216 (2008), doi: 10.1086/533487
- [5] Ch. C. Moustakidis, T. Gaitanos, Ch. Margaritis and G. A. Lalazisis, Phys. Rev. C 95, 045801 (2017), doi: 10.1103/PhysRevC.95.045801
- [6] S. Postnikov, M. Prakash, and J. M. Lattimer, Phys. Rev. D 82, 024016 (2010), doi: 10.1103/PhysRevD.82.024016
- [7] T. Hinderer, B. D. Lackey, R. N. Lang and J. S. Read, Phys. Rev. D 81, 123016(2010), doi: 10.1103/PhysRevD.81.123016
- [8] S. De et al. , Phys.Rev. Lett. 121, 091102 (2018), doi: 10.1103/PhysRevLett.121.091102
- [9] D. Radice, A. Perego, F. Zappa, S. Bernuzzi, Astrophys. J. 852, L29 (2018), doi: 10.3847/2041-8213/aaa402
- [10] T. Zhao, J.M. Lattimer, Phys. Rev. D 98, 063020 (2018), doi: 10.1103/PhysRevD.98.063020
- [11] B. P. Abbott et al., Phys. Rev. Lett. 121, 161101 (2018), doi: 10.1103/PhysRevLett.121.161101
- [12] B. P. Abbott et al., Physical Review X 9, 011001 (2019), doi: 10.1103/PhysRevX.9.011001